Deformation behaviour of re-entrant carbon honeycomb structures

L Kh Rysaeva[1], A I Klyavlina[2], F Kh Galiachmetov[1], J A Baimova[1,2], D S Lisovenko[3] and V A Gorodtsov[3]
[1]Institute for Metals Superplasticity Problems of the Russian Academy of Sciences, Khalturina 39, Ufa 450001, Russia
[2]Bashkir State University, Validy Str. 32, Ufa 450076, Russia
[3]Ishlinsky Institute for Problems in Mechanics of the Russian Academy of Sciences, Prospekt Vernadskogo 101-1, Moscow 119526 Russia

E-mail: lesya813rys@gmail.com

Abstract. Recent successes of researchers in the fabrication of new carbon structures of different morphologies and dimensions open up broad prospects for the development of carbon materials with qualitatively new properties. Such promising materials are cellular structures (or carbon aerogels) that have high deformability, good adsorption and conductivity characteristics. In this work, we consider a carbon structure consisting of re-entrant honeycomb cells, which allow the structure to be auxetic. The stability and deformation behaviour of re-entrant carbon honeycomb structures is studied by molecular dynamics simulation. The effect of structural parameters on the stability of carbon aerogel is discussed. It is shown that structural changes significantly depend on the strain rate and the loading direction. At a high strain rate in tension along the *z*-axis, all cells open slightly at the same time. On the contrary, at small strain rates, certain cells open, while others almost completely collapse, which is expected to result in changes in physical properties, for example, in conductivity. During tension along the *x*-axis, a transformation from a re-entrant honeycomb to a traditional honeycomb took place.

1. Introduction

Various carbon nanostructures with complex geometries are of great interest because of novel physical, mechanical and electronic properties. Very promising results have been obtained for three-dimensional carbon structures of different morphologies, such as crumpled graphene [1, 2, 3], carbon aerogels [4], peapods [5], diamond-like phases [6, 7] etc. Graphene aerogels or cellular honeycomb structures comprise a promising new class of materials, since they exhibit nanoscale mechanical properties of graphene, while also achieve new properties that can be tuned by designing their morphology. Among such structures, cellular materials based on graphene flakes are of interest [4, 8, 9, 10]. The idea of creating such morphology is quite simple and inspired by the morphology of graphene itself - carbon atoms stacked in a hexagonal lattice. As it was shown experimentally [8, 11], these structures are stable and can be obtained on the basis of graphite. One of the important advantages of aerogel structures is a high rate of gas adsorption, which makes it possible to predict their usage in the storage and transportation of hydrogen [8, 11, 12]. In addition to chemical

properties, their mechanical properties play an important role in the use of cellular structures in various nanodevices. For example, it was shown that cellular structures exhibit unique strength and ultra-high extensibility [10, 13, 14].

These structures can be presented, for instance, as a system of stacked graphene nanoribbons. Among the previously studied carbon aerogels are structures with square [4] and honeycomb [8, 11, 12] cells, while many other opportunities to combine graphene nanoribbons to a complex architecture are not considered.

In the present work, the effect of structural features on the stability of the re-entrant honeycomb cellular structure is investigated by molecular dynamics (MD) simulation. The simulation is carried out to study the deformation behaviour of this structure under one-dimensional tensile loading.

2. Simulation details

The initial structure of re-entrant honeycomb cells is created using a specially developed code that allows combining nanoribbons into a structure with the main required parameters such as the angle of inclination θ, the size of the cell sides l, h and the width of the nanoribbon a.

Figure 1 a shows a part of the initial structure with the main geometrical parameters. To create a cellular structure, a carbon nanoribbon of the "armchair" type is chosen. When constructing the simulation cell, the following parameters were used: $\theta = 60^o$ and $l/h = 0.5$. These parameters were proposed in [15], where auxetic materials (i.e. materials with a negative Poisson's ratio [16, 17, 18]) of the same structural configuration were investigated. Values of the nanoribbon width in the y direction from 12 Å to 60 Å are considered. It is found that no significant changes in the relaxation behavior of the structures occur. Thus, a = 12 Å is considered below.

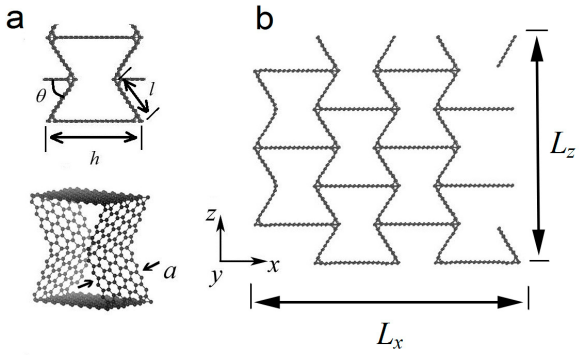

Figure 1. An example of a cellular structure (a) is the elementary cell in the projection onto the xz plane and in perspective (θ is the slope angle, h and l are the sides length, and a is the nanoribbon width), (b) the periodicity cell used in the projection on to the xz plane.

All the structures and their properties have been studied using the freely distributed program package LAMMPS with the interaction between carbon atoms defined by the well known interatomic interaction potential AIREBO [19]. Periodic boundary conditions are applied to the x, y and z directions. The periodicity cell in projection to the xz plane is shown in figure 1 b. At first, the structure is minimized for 20 ps to an equilibrium state with a minimal potential energy. A Nose-Hoover thermostat is used with a target temperature of 1 K with a constant number of atoms and standard velocity-Verlet time integration with a timestep of 1 fs.

To study the deformation behaviour, the uniaxial tensile stress $\sigma_x(\sigma_z)$ is applied to the structure along the x or z axes and the corresponding stress components $\sigma_z(\sigma_x)$ are calculated. The range of elongation rates $\dot{\varepsilon}$ from 2 Å/ps to 0.1 Å/ps is considered, but only two typical elongation rates are presented: $\dot{\varepsilon} = 1$ Å/ps and $\dot{\varepsilon} = 0.1$ Å/ps. The length of the simulation cell L_z (L_x) along the $z(x)$-axis allows one to find the final strain $\varepsilon = (L_{z(\text{final})}\text{-}L_{z(0)})/L_{z(0)}$ and track the change in the cell size. The stress component σ_y does not change in the process of deformation, remaining close to zero. The stress component σ_z for tension along z - axis and σ_x for tension along the x - axis changes linearly during the deformation process. Therefore, $\sigma_z(\sigma_x)$ and σ_y are not presented.

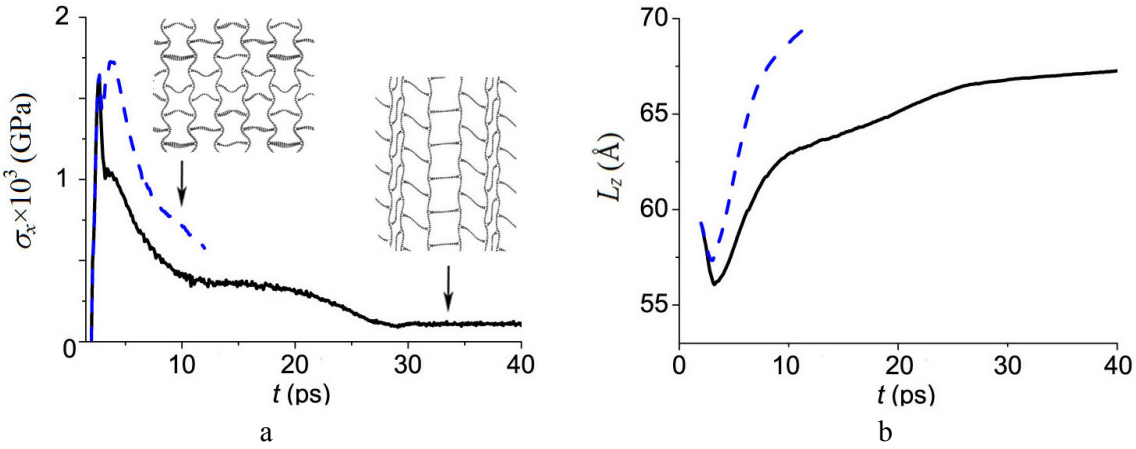

a b

Figure 2. The stress σ_x (a) and the length of the simulation cell along the z axis (b) as a function of time for two strain rates: $\dot{\varepsilon} = 0.1$ Å/ps (black solid line) and $\dot{\varepsilon} = 1$ Å/ps (blue dashed line).

3. Results and discussion

3.1. Tension along z direction

In figures 2 a, b, the stress σ_x and the length of the simulation cell along the z axis are presented as a function of time for $\dot{\varepsilon} = 1$ Å/ps and $\dot{\varepsilon} = 0.1$ Å/ps. As can be seen from figure 2 a, a sharp increase in the stresses σ_x occurs during the first 2 ps, which is typical for all deformation rates. The growth of stresses along the x axis until 2 ps is accompanied by a slight decrease in the cell size in the z-axis which means the relaxation process. After 2 ps, a gradual relaxation of σ_x takes place for at least 20 ps. The structure of re-entrant honeycomb in the projection to the xz plane after deformation at two strain rates, shown by arrows on the graph, is presented in figure 2 a. At high strain rates (1 Å/ps), the structure is stretched uniformly, while at small strain rates ($\dot{\varepsilon} = 0.1$ Å/ps), the deformation occurs non-uniformly in each layer, which leads to a transformation of the structure - some cells open and others collapse. Reducing the strain rate leads to the relaxation of stresses during the stretching process. For $\dot{\varepsilon} = 0.1$ Å/ps, both covalent and Van-der-Waals interactions are taken into account, since atoms in a slower regime can easily interact with the neighbors that is close to the structural relaxation. It can be concluded that at too high strain rates such relaxation does not occur, which has an effect on the final result. As a result, it is possible to obtain a structure with the required parameters (uniformly or non-uniformly stretched cells).

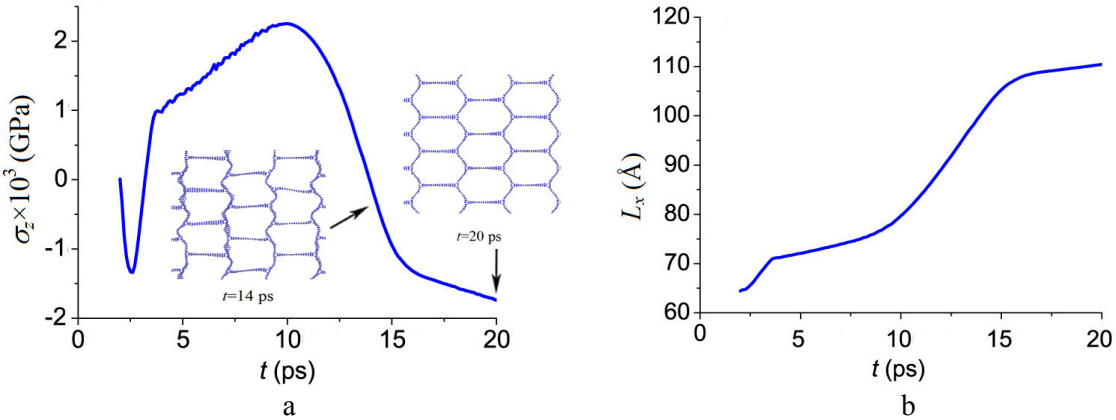

a b

Figure 3. The stress σ_z (a) and the length of the simulation cell along the x axis (b) as a function of time for $\dot{\varepsilon} = 2.3$ Å/ps.

3.2. Tension along x direction

Here, the behavior of the structure under uniaxial tension along the *x*-axis is presented for $\dot{\varepsilon} = 2.3$ Å/ps. In figures 3a, b, σ_z and the size of the simulation cell along *x*-axis as a function of time is shown. The corresponding structural states during deformation are also shown in figure 3 a. As it can be seen, re-entrant honeycombs transform to squares in about 13-14 ps, and then to traditional honeycomb cells after tension in 16-17 ps. In the initial state, before 2 ps, the relaxation of the structure takes place, while after that an abrupt increase of the stress can be seen, which is connected with the transformation of are-entrant honeycomb to its traditional form as described above. After transformation to almost square cells (at about 10 ps), the stress relaxation can be seen (for 11-15 ps). Then, all structural changes are completed, and further deformation will lead to a fraction of the carbon aerogel.

4. Conclusions

To summarize, MD simulations are performed to investigate the stability and deformation behavior of the class of graphene superstructure aerogels with an emphasis on structural parameters. The most favourable angle of inclination, equal to $\theta = 60°$ with a favourable ratio *l/h,* equal to 0.5, is chosen. It is shown that the width of the nanoribbon at periodic boundary conditions has no effect on the stability and properties of the honeycomb structure at periodic boundary conditions.

It is noted that the deformability of the structure depends on the strain rate. At too small strain rates, uniformly stretched cells appear, while tension along the *z*-axis with a high strain rate leads to a redistribution of stresses in the structure and the formation of a banded morphology, where two types of cells are obtained. The tension along the *x*-axis leads to the transformation of the re-entrant honeycombs to the stretched honeycomb cells.

Acknowledgments

Initial simulation setup was conducted by D.S.L. and V.A.G. and supported by RFBR, grant 16-01-00325 and Government Assignment AAAA-A17-117021310373-3. Stability analysis was conducted by J.A.B. and supported by grant of the President of the Russian Federation for state support of young Russian scientists MD-1651.2018.2. Calculations were conducted by R.L.Kh. and supported by the RSF, grant 14-13-00982. Work is conducted in the frame of the program of fundamental researches of Government Academy of Sciences of IMSP RAS.

References

[1] Korznikova E A, Baimova J A, Dmitriev S V, Korznikov A V and Mulyukov R R 2014 *Rev. Adv. Mater. Sci.* **39** 92
[2] Baimova J A, Korznikova E A, Dmitriev S V, Liu B and Zhou K 2014 *Rev. Adv. Mater. Sci.* **39** 69
[3] Baimova J A, Liu B, Dmitriev S V, Srikanth N and Zhou K 2014 *Phys. Chem. Chem. Phys.* **16** 19505
[4] Morris B, Becton M and Wang X 2018 *Carbon* **137** 196
[5] Katin K P, Prudkovskiy V S and Maslov M M 2016 *Physica E* **81** 1
[6] Belenkov E A and Greshnyakov V A 2017 *Letters on Materials* **7** 318
[7] Belenkov E A, Brzhezinskaya M M and Greshnyakov V A 2014 *Diam. Rel. Mater.* **50** 9
[8] Krainyukova N V 2016 *J. Low Temper. Phys.* **187** 90
[9] Wu M, Wu X, Pei Y, Wang Y and Zeng X C 2011 *Chem. Commun.* **47** 4406
[10] Zhang Z, Kutana A, Yang Y, Krainyukova N V, Penev E S and Yakobson B I 2017 *Carbon* **113** 26
[11] Krainyukova N V and Zubarev E N 2016 *Phys. Rev. Lett.* **116** 055501
[12] Antipina L Y, Avramov P V, Sakai S, Naramoto H, Ohtomo M, Entani S, Matsumoto Y and Sorokin P B 2012 *Phys. Rev. B* 86 085435
[13] Pang Z, Gu X, Wei Y, Yang R and Dresselhaus M S 2016 *Nano Lett.* **17** 179

[14] Gu X, Pang Z, Wei Y and Yang R 2017 *Carbon* **119** 278
[15] Grima J N, Oliveri L, Attard D, Ellul B, Gatt R, Cicala G and Recca G 2010 *Adv. Eng. Mater*. **12** 855
[16] Goldstein R V, Lisovenko D S, Chentsov A V and Lavrentyev S Y 2017 *Letters on Materials* **7** 81
[17] Goldstein R V, Gorodtsov V A and Lisovenko D S 2016 *Phys. Status Solidi B* **253** 1261
[18] Goldstein R V, Gorodtsov V A, Lisovenko D S and Volkov M A 2015 *Letters on Materials* **5** 409
[19] Stuart S J, Tutein A B and Harrison J A 2000 *J. Chem. Phys*. **112** 6472